



1 Composition, size and cloud condensation nuclei activity of biomass burning aerosol
2 from north Australian savannah fires.

3 **Authors:**

4 Marc D. Mallet¹, Luke T. Cravigan¹, Anđelija Milic¹, Joel Alroe¹, Zoran D. Ristovski¹,
5 Jason Ward², Melita Keywood², Leah R. Williams³, Paul Selleck², Branka Miljevic^{1*}

6 **Affiliations:**

7 ¹School of Chemistry, Physics and Mechanical Engineering, Queensland University of Technology,
8 Queensland, Brisbane, 4001, Australia

9 ²CSIRO Oceans and Atmosphere Flagship, Aspendale, Victoria, 3195, Australia

10 ³Aerodyne Research, Inc., Billerica, Massachusetts, 01821, USA

11 **Corresponding author:**

12 Dr Branka Miljevic

13 Contact Phone: +71 7 3138 3827

14 Contact Email: b.miljevic@qut.edu.au



1 **Abstract**

2 The vast majority of Australia's fires occur in the tropical north of the continent during
3 the dry season. These fires are a significant source of aerosol and cloud condensation
4 nuclei (CCN) in the region, providing a unique opportunity to investigate the biomass
5 burning aerosol (BBA) in the absence of other sources. CCN concentrations at 0.5%
6 supersaturation and aerosol size and chemical properties were measured at the
7 Australian Tropical Atmospheric Research Station (ATARS) during June 2014. CCN
8 concentrations reached over 10^4 cm^{-3} when frequent and close fires were burning; up
9 to 45 times higher than periods with no fires. Both the size distribution and composition
10 of BBA appeared to significantly influence CCN concentrations. A distinct diurnal
11 trend in the proportion of BBA activating to cloud droplets was observed, with an
12 activation ratio of $40\% \pm 20\%$ during the night and $60\% \pm 20\%$ during the day. BBA
13 was, on average, less hygroscopic during the night ($\kappa = 0.04 \pm 0.03$) than during the
14 day ($\kappa = 0.07 \pm 0.05$), with a maximum typically observed just before midday. Size-
15 resolved composition of BBA showed that organics comprised a constant 90% of the
16 aerosol volume for aerodynamic diameters between 100 nm and 200 nm. The
17 photochemical oxidation of organics led to an increase in the hygroscopic growth and
18 an increase in daytime activation ratios. Modelled CCN concentrations assuming
19 typical continental hygroscopicities produced very large overestimations of up to
20 200%. Smaller, but still significant over predictions up to $\sim 100\%$ were observed using
21 AMS and H-TDMA derived hygroscopicities as well as campaign night and day
22 averages. The largest estimations in every case occurred during the night when the
23 small variations in very weakly hygroscopic species corresponded to large variations
24 in the activation diameters. Trade winds carry the smoke generated from these fires
25 over the Timor Sea where aerosol-cloud interactions are likely to be sensitive to
26 changes in CCN concentrations, perturbing cloud albedo and lifetime. Dry season fires
27 in north Australia are therefore potentially very important in cloud processes in this
28 region.

29 **1 Introduction**

30 Biomass burning aerosol (BBA) can act as efficient cloud condensation nuclei (CCN)
31 and form cloud droplets. Fires can therefore influence cloud formation, growth,
32 reflectance, precipitation and lifetime (Kaufman et al., 1998; Warner and Twomey,
33 1967). The contribution of CCN from fires results in higher concentrations of cloud



1 droplets, which yield whiter clouds that generally survive longer than clouds with fewer
2 droplets (Platnick and Twomey, 1994). While greenhouse gases and black carbon
3 emitted from fires absorb radiation and have a warming effect, the influence of solar
4 radiation scattering by organic material and the production of CCN has a cooling effect
5 on the Earth's lower atmosphere. The net forcing of carbonaceous combustion aerosol
6 is thought to have an overall global cooling effect (Spracklen et al., 2011; Ward et al.,
7 2012). The complexity arises from variability in emission factors, BBA size,
8 composition and aging, and contributes to a large uncertainty that these fires have on
9 the radiative budget (Carslaw et al., 2010). Thus detailed measurements of the physical
10 and chemical properties of BBA from all regions in different seasons are essential in
11 determining their impact on clouds (Spracklen et al., 2011). Very few studies have
12 taken place within Australia, despite Australia contributing an estimated 15% of yearly
13 global burned land area (van der Werf et al., 2006). Australian studies have been
14 typically focused on fires in the southern continent (Lawson et al., 2015) or east coast
15 cane fires (Warner and Twomey, 1967). The extent to which dry season fires in north
16 Australia impact CCN concentrations has not been explored in detail.

17
18 Most of central north Australia is unpopulated and is characterized by savannah
19 vegetation. The vast majority of Australia's fires occur in this region. During the dry
20 season (May until November) thousands of fires burn via prescribed burning and
21 spontaneous or accidental ignitions. The frequency and severity of these fires increases
22 as the season progresses from the early dry season to the late dry season (Andersen et
23 al., 2005). Under Aboriginal management, fires were lit in the late dry season in order
24 to prepare for the wet season. These late dry season fires may have been lit intentionally
25 to trigger the onset of rainfall following the formation of pyro-cumulus clouds, among
26 other ecological reasons (Bowman and Vigilante, 2001; Bowman et al., 2007). Under
27 non-Indigenous management, early dry season prescribed burns are commonplace in
28 order to reduce the severity of late dry season fires (Andersen et al., 2005). Outside of
29 the only major urban center in this region, Darwin, prescribed burns are the dominant
30 source of accumulation mode aerosol particles (Mallet et al., 2016, submitted). Thus
31 these prescribed burns will dictate CCN concentrations in the region.

32



1 The vegetation (fuel) type, burning conditions and atmospheric aging determines the
2 size, composition and the hygroscopicity of BBA, and in turn their ability to act as
3 CCN. BBA is typically a mixture of elemental carbon, organic carbon and can contain
4 inorganic material (Reid et al., 2005). The precise organic carbon composition of
5 primary BBA can vary greatly depending on the fuel type and these organic constituents
6 can be weakly or highly hygroscopic (Carrico et al., 2010; Mochida and Kawamura,
7 2004; Novakov and Corrigan, 1996; Petters et al., 2009). The hygroscopicity of BBA
8 can change with oxidation and with the condensation or evaporation of volatile organic
9 compounds (VOCs) through atmospheric aging (Hennigan et al., 2011). Smog chamber
10 experiments have shown that after a few hours of simulated photochemical aging, the
11 hygroscopicity of BBA converges to weakly hygroscopic for many different fuel types
12 (Engelhart et al., 2012; Giordana et al., 2013).

13

14 While laboratory based measurements are useful in understanding the physical and
15 chemical processes that can occur that determine the hygroscopicity and composition
16 of aerosol, they do not necessarily represent ambient conditions. Due to feasibility,
17 however, direct ambient measurements of the CCN activity of smoke plumes are rare
18 (Lawson et al., 2015) and more measurements are useful in assessing the validity of
19 climate models. A previous preliminary study of the CCN activity of savannah fires in
20 the north Australian early dry season reported moderately hygroscopic BBA (Fedele,
21 2015), speculating that the aerosol is mostly made up of aged biomass burning particles
22 with a coating of secondary organic aerosol. While these measurements took place over
23 a short period, there was a discernable slight increase in the hygroscopicity of BBA
24 during the day. Diurnal patterns in hygroscopicity have been observed in boreal
25 environments (Paramonov et al., 2013) and in the southeast United States (Cerully et
26 al., 2015), attributing increases in daytime hygroscopicity to the photochemical
27 oxidation of organic aerosol.

28

29 Some studies suggest that the impact of composition, and therefore changes in BBA
30 hygroscopicity due to photochemical aging, on CCN concentrations is much lower than
31 the impact from the aerosol size distribution (Dusek et al., 2006; Petters et al., 2009;
32 Spracklen et al., 2011). Under this assumption, changes to the activation diameter
33 resulting from a change in hygroscopicity are less important than the size distribution
34 of the BBA. Other studies have shown that while this is true for moderately and strongly



1 hygroscopic particles, cloud droplet number concentrations are moderately sensitive to
2 weakly hygroscopic particles (Reutter et al., 2009; Gacita et al., 2016).

3
4 Smoke from biomass burning can be transported over intercontinental distances and
5 can reach the upper levels of the atmosphere (Andreae et al., 2001; Dirksen et al., 2009).
6 Aircraft measurements during the early and late dry season in north Australia, however,
7 suggest that smoke from fires in this region are contained within the planetary boundary
8 layer (Ristovski et al., 2010; Kondo et al., 2003). Trade winds collect and carry this
9 smoke northwest over northern Australia, the Timor Sea and the tropical warm pool.
10 Cloud albedo is more sensitive to aerosol concentrations in pristine environments
11 (Twomey, 1991). The biomass burning that occurs during the dry season is the
12 dominant source of particles in north Australia, and is therefore likely to influence
13 aerosol-cloud interactions over the tropical warm pool in the Timor Sea.

14
15 This paper presents a comprehensive data set of the particle size, chemical composition,
16 hygroscopicity and CCN properties of BBA generated from fires in the dry season in
17 this region. The impact of BBA size and hygroscopicity on CCN activation are
18 discussed in detail. These parameters will be useful in climate models to assess the
19 magnitude of climate forcing by BBA in aerosol-cloud interactions.

20 **2 Experimental**

21 Sampling took place at the Australian Tropical Atmospheric Research Station
22 (ATARS; 12°14'56.6"S, 131°02'40.8"E), Gunn Point, in the Northern Territory of
23 Australia as a part of the Savannah Fires in the Early Dry season (SAFIRED) campaign
24 (Mallet et al., 2016). The research station is located near the tip of a small peninsula
25 with close proximity to the Timor Sea and Tiwi Islands. The Territory capital, Darwin,
26 lies 20 km to the south west of the station. Savannah vegetation with scarce human
27 settlements transition over hundreds of kilometers to the south into the desert regions
28 of central Australia. Sampling for the SAFIRED campaign occurred in June 2014 at
29 ATARS. This period is the early dry season in this region, where strategic small-scale
30 controlled burns are performed in order to reduce the frequency and intensities of fires
31 in the late dry season in October and November. Despite sampling occurring during
32 winter, daily temperatures can reach well above 30°C such that accidental and natural
33 fires can also occur. Throughout the sampling period, thousands of fires were observed



1 in northern Australia. This led to strong biomass burning signatures detected at the
2 station, with numerous instances of very intense BBA events from both distant and
3 close fires. A full overview of the campaign, including meteorological, gaseous and
4 aerosol measurements is presented in Mallet et al. (2016, submitted).

5
6 Sentinel Hotspots, an Australian national bushfire monitoring system, was used to
7 investigate the number of daily fires in the region. Sentinel uses data from the MODIS
8 (Moderate-resolution Imaging Spectroradiometer) sensors onboard the Terra and Aqua
9 NASA satellites and the VIIRS (Visible Infrared Imaging Radiometer Suite) sensor
10 onboard the NASA/NOAA Suomi NPP satellite. These satellites fly over north
11 Australia once per day between 11:00 am and 3:00 pm local time. Although fire
12 locations are therefore limited to those that are burning during these times, Sentinel is
13 still useful in providing information on the spread and number of fires burning in the
14 region. For this study, the total number of observed fires within 20 km and 50 km of
15 ATARS were calculated (Figure 1b) for a qualitative assessment of how the smoke
16 from these fires can affect cloud condensation nuclei concentrations.

17

18 **2.1 Instrumentation**

19 Aerosol size, concentration, composition, hygroscopicity and CCN concentration
20 measurements were taken to characterise BBA water uptake and its potential impact on
21 cloud formation. Ambient aerosol was sampled through an automated regenerating
22 aerosol diffusion dryer to condition the intake to below 40% relative humidity. PM₁
23 filters were collected on a TAPI 602 Beta plus particle measurement system (BAM) for
24 an analysis of elemental and organic carbon. A Scanning Mobility Particle Analyzer
25 (SMPS) made up of a TSI 3071 electrostatic classifier and TSI 3772 Condensation
26 Particle Counter (CPC) was used to determine the particle size distributions and number
27 concentrations between 14 nm and 650 nm with a 5 minute averaging time. A Cloud
28 Condensation Nuclei Counter (CCNC) was used to measure total cloud droplet
29 concentrations at a supersaturation of 0.5% every 10 seconds. A Hygroscopicity
30 Tandem Differential Mobility Analyser (H-TDMA) alternated measurement of the
31 hygroscopic growth factor (HGF; D/D_0) of ambient 50 and 150 nm size selected
32 particles exposed to a relative humidity of 90% (Johnson et al., 2004).

33



1 An Aerodyne compact Time-of-Flight Aerosol Mass Spectrometer (cToF-AMS) was
2 used to determine the size-resolved chemical composition of non-refractory sub-micron
3 aerosol. A full discussion on the cToF-AMS analysis of the composition of bulk PM₁
4 aerosol can be found in Milic et al. (2016). Briefly, in order to account for fragmentation
5 table issues during periods of high signals in which some sulphate species were
6 misattributed to organics, the high-resolution AMS analysis toolkit, PIKA, was used to
7 separate organic and sulphate signals. Data for the analysis of the size-resolved
8 chemical composition within PIKA were not recorded during the sampling period and
9 therefore the standard AMS analysis toolkit, Squirrel, was used with unit mass
10 resolution. In order to account for fragmentation table issues related to the incorrect
11 assignment of organic and sulfate species, the size-resolved mass concentrations for
12 each species were scaled by the ratio of the mass concentrations reported by the PIKA
13 analysis to the integrated mass concentrations reported by Squirrel. The size-resolved
14 composition revealed that inorganic ammonium and sulphate species made up a greater
15 contribution of larger particles than in smaller particles (Figure S1). The composition
16 of particles between 100 nm and 200 nm (aerodynamic diameter) was therefore used in
17 this study as this size range is more representative of aerosols at the CCN activation
18 diameter. This is further discussed in section 3.3.

19

20 2.2 Analysis

21 Total particle number concentrations (PNc) were calculated by integrating the size
22 distributions measured by the SMPS. The activation ratio of BBA as CCN at 0.5%
23 supersaturation was calculated by dividing the CCN_c by the PNc. Apparent activation
24 diameters were calculated by a step-wise integration of the particle size distribution
25 from the maximum size bin towards the lower size bins until the total number of
26 particles exceeded the total number of CCN, as per:

$$CCN_c = \int_{Activation\ diameter}^{Upper\ diameter} dN/d\log D_p \cdot dD_p \quad \text{Equation 1}$$

27 where CCN_c is the total cloud condensation nuclei concentration, N is the particle
28 number concentration for each size bin, D_p is the particle diameter, the upper diameter
29 is the largest size measured by the SMPS (650 nm) and the activation diameter is the
30 size at which the particles activate to cloud droplets. To calculate the precise activation
31 diameter, a linear fit ($R^2 > 0.98$) between the cumulative particle number concentrations
32 and the diameter was applied across 11 size bins centered on the bin in which the



1 activation diameter falls. The uncertainty in the activation diameters was calculated
2 assuming a maximum uncertainty in the CCN concentrations of $\pm 10\%$ and was
3 typically of the order of 7 nm.

4

5 The apparent activation diameters were then used to calculate the average effective
6 hygroscopicity parameter, κ , for each SMPS scan following κ -Kohler theory (Petters
7 and Kreidenweis, 2007; Petters et al., 2009). According to this theory, the
8 supersaturation required to achieve a particular droplet diameter for any given particle
9 can be determined using:

$$S(D) = \frac{D^3 - D_d^3}{D^3 - D_d^3(1 - \kappa)} \exp\left(\frac{4\sigma_{s/a}M_w}{RT\rho_w D}\right) \quad \text{Equation 2}$$

10 where S is the supersaturation, D is the droplet diameter, D_d is the dry particle diameter,
11 κ is the hygroscopicity parameter, $\sigma_{s/a}$ is the surface tension of the interface between
12 the solution and air (typically 0.072 J m^{-2} as pure water is assumed), M_w is the molecular
13 weight of water, R is the universal gas constant, T is the temperature (taken as $308 \text{ K} \pm$
14 3 K in this study) and ρ_w is the density of water. For a range of D_d values, κ and D
15 values were iteratively varied until the maximum of the κ -Kohler curve was equal to
16 0.5% , the supersaturation used in the CCNC. A relationship was then found between κ
17 and D_d for the range of 45 nm up to 160 nm (Figure S2). This relationship was then
18 applied to the calculated activation diameters over the sampling period to calculate the
19 BBA κ values. The uncertainty in the activation diameter of 7 nm led to a uncertainties
20 in κ of ~ 0.05 for activation diameters between 60 nm and 80 nm, ~ 0.01 for activation
21 diameters between 80 nm and less than 0.01 for activation diameters above 100 nm.

22

23 The value of κ derived from the CCNC and SMPS is the average for all particle sizes.
24 If there is not a uniform composition, this value cannot necessarily be applied to all
25 sizes of BBA. All H-TDMA data were inverted using the TDMAinv algorithm (Gysel
26 et al., 2009) and HGF distributions were kelvin-corrected for comparison between 50
27 and 150 nm particles at 90 % relative humidity. Equation 2 was then also applied to the
28 kelvin corrected HGF distributions, thereby providing distributions of κ . This also
29 provides an insight into the mixing state of the BBA, which cannot be determined from
30 the CCNC and SMPS measurements in this study.

31



1 When the surface tension of pure water is assumed, κ is regarded as the "effective
2 hygroscopicity parameter", which accounts for changes in water activity due to the
3 solute as well as any surface tension effects (Petters and Kreidenweis, 2007; Rose et al.,
4 2010; Pöschl et al., 2009). The effective hygroscopicity parameter is therefore an
5 indication of all compositional effects of an aerosol particle on water uptake. To
6 distinguish the potential effects of surface tension, values of 0.052 J m^{-2} and 0.0683 J
7 m^{-2} were also applied. Mircea et al. (2005) suggest that the surface tension at the liquid-
8 air interface of a particle depends on the concentration of carbon. The value 0.052 J m^{-2}
9 2 represents a lower limit while a surface tension of 0.0683 J m^{-2} has been observed for
10 prescribed biomass burning particulate matter in wooded areas in the USA (Asa-Awuku
11 et al., 2008). The impact of surface tension is discussed further in Section 3.5.

12

13 The overall hygroscopicity of any given particle can be determined by the volume
14 fraction and hygroscopicity of each constituent under the Zdanovskii, Stokes and
15 Robinson assumption (Chen et al., 1973; Stokes and Robinson, 1966):

$$\kappa = \sum_i \varepsilon_i \kappa_i \quad \text{Equation 3}$$

16 where κ is the overall hygroscopicity and ε_i and κ_i are the volume fractions and
17 hygroscopicities of each constituent, respectively. A modelled κ was constructed to
18 determine the influence of diurnal changes in organic and inorganic volume fractions,
19 where $\kappa_{\text{total}} = \varepsilon_{\text{org}} \kappa_{\text{org}} + \varepsilon_{\text{EC}} \kappa_{\text{EC}} + \varepsilon_{\text{inorganic}} \kappa_{\text{inorganic}}$, following the ZSR assumption. The 12-
20 hour PM₁ BAM filters sampled from 07:00 until 19:00 (day) and from 19:00 until 07:00
21 (night) each day showed no difference in the ratio of EC to (OC + EC), and therefore a
22 constant mass fraction (EC/(EC + OC)) of 10% was applied. ε_{org} , ε_{EC} and $\varepsilon_{\text{inorganic}}$ were
23 calculated using the size-resolved mass concentrations reported by the cToF-AMS and
24 assumed densities of 1.4 g cm^{-3} (Levin et al., 2014), 1.8 g cm^{-3} (Bond and Bergstrom,
25 2006) and 1.8 g cm^{-3} (Levin et al., 2014), respectively. $\kappa_{\text{inorganic}}$ and κ_{EC} were taken as
26 0.60 (Bougiatioti et al., 2016) and 0 (Petters and Kreidenweis, 2007), respectively. A
27 night (18:00 until 07:00) and day value of κ_{org} were varied in the applied model in order
28 to investigate any potential changes in organic hygroscopicity due to photochemistry.

29

30 CCN concentrations were calculated in order to test prediction of CCN concentrations
31 using aerosol composition and size distribution in this region. Activation diameters
32 were derived from various hygroscopicity parameters and, again using Equation 1, the



1 size distribution was integrated step-wise from the upper size limited measured in the
2 SMPS until the activation diameter was reached. The same process used to calculate
3 the precise activation diameters earlier was used to calculate the precise CCN
4 concentrations. This process was carried out for the modelled hygroscopicity from the
5 size-resolved cToF-AMS data, the measured hygroscopicity distribution from the H-
6 TDMA as well as various constant hygroscopicity values. The constant values selected
7 were 0.05, 0.1, 0.2, 0.3 and a day and night value of 0.071 and 0.035, respectively. 0.05
8 represents the campaign average effective hygroscopicity. The day and night values
9 represent the campaign average values obtained from the SMPS-CCNC measurements.
10 The values of 0.1 and 0.2 represent commonly observed hygroscopicities for BBA in
11 other regions and in laboratory measurements Engelhart et al. (2012). The global mean
12 values of κ have been estimated to be 0.27 ± 0.21 for continental aerosols (Pringle et
13 al., 2010). It has been suggested that it is suitable to assume this continental average (κ
14 ~ 0.3) to make first order predictions of CCN activity (Rose et al., 2011). Modelling
15 CCN concentrations using these methods and assumed hygroscopicity values will
16 verify whether such values are suitable in predicting CCN activity in regions like
17 northern Australia.

18

19 In order to investigate the CCN activity of BBA, four days of unpolluted and coastal
20 conditions (19/06/2014 - 22/06/2014) were removed from the majority of the analysis.
21 Furthermore, the SMPS was only operational from 04/06/2014. Analysis of CCNc,
22 PNc, activation ratios, median particle diameters, apparent activation diameters and the
23 average effective hygroscopicity parameters are therefore only presented for data
24 collected after this date.

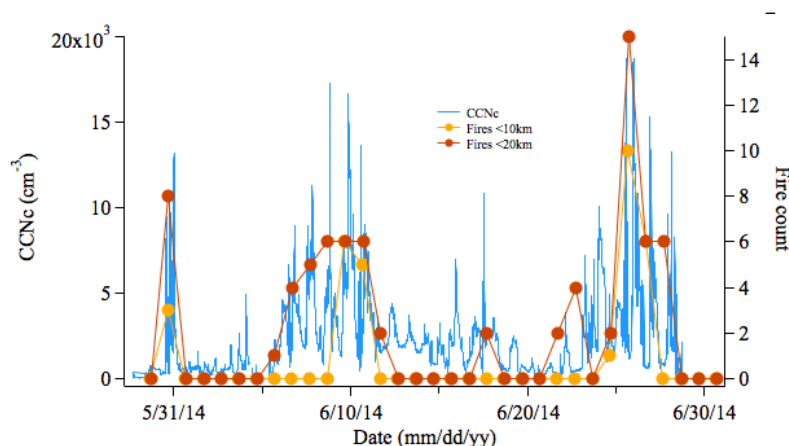
25 **3 Results and Discussion**

26 **3.1 BBA contribution to CCN**

27 Figure 1 shows the CCN concentrations (SS 0.5%) measured at the ATARS over the
28 campaign sampling period in June 2014 as well as the frequency of fires that were
29 observed via satellite hotspots each day within 20 km and 50 km of the station. Air
30 mass back trajectories were typically from the southeast, as were the location of the
31 fires (Mallet et al., 2016). The period between the 19th and 23rd of June was
32 characterized by relatively low CCN concentrations due to air originating from the
33 coastal waters of eastern Australia, which passed over minimal continental area before



1 arriving at the ATARS. As already mentioned, these dates were subsequently excluded
2 from the data analysis as the focus of this study was on the impact of BBA on CCN.
3 The highest PNC and CCN concentrations were associated with large BB events. PNC
4 concentrations of up to 400000 cm^{-3} and CCN concentrations of up to 18000 CCN cm^{-3}
5 were observed during these periods.
6



17

18 *Figure 1* The time series of a) total cloud condensation nuclei concentrations (CCN) at 0.5% supersaturation and
19 b) the total number of fires satellite-observed fires within 20 km (red) and 50 km (green) of the sampling location.

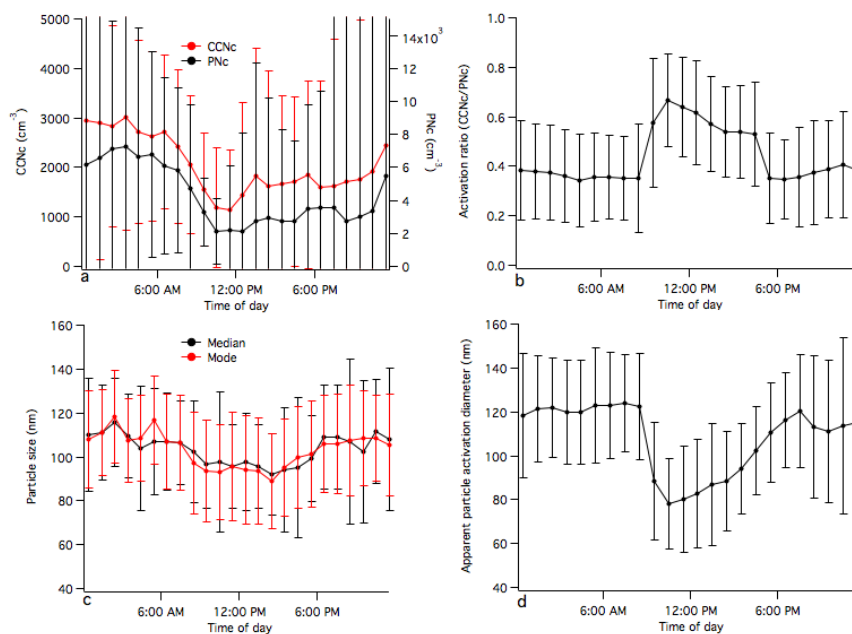
20 Although the PNC and CCN concentrations were highest during BBA events, these
21 periods were characterized by the lowest hygroscopicity and activation ratios (ratio of
22 CCNc to PNC as low as 4%). This is further discussed in Section 3.3. Activation ratios
23 typically varied between 30% and 80%, corresponding to CCN concentrations between
24 1500 cm^{-3} and 6000 cm^{-3} . This contrasts observed activation ratios of over 80% in BBA
25 from dry season savannah fires in tropical southern Africa during the SAFARI 2000
26 campaign (Ross et al., 2003), despite lower supersaturations of $\sim 0.3\%$. The size
27 distributions of BBA observed during SAFIRED had a count median diameter of 107
28 $\text{nm} \pm 25\text{ nm}$, while the median diameters were typically above 150 nm in the SAFARI
29 2000 campaign, which could explain the lower activation ratios observed here. The size
30 distributions observed in this study were typically smaller than those observed in aged
31 and regional BBA on other continents (Reid et al., 2005). When particles are smaller,
32 the critical diameter for cloud droplet formation becomes more important. It is therefore
33 crucial to investigate the impact of composition on the activation diameter, and thus
34 CCN concentrations.



1

2 3.2 Diurnal trends in BBA

3 Diurnal patterns in the BBA PNc, CCNc, size and activation ratio and activation
4 diameter are shown in Figure 2. For most of the campaign, particle size distributions
5 were unimodal and therefore the median and mode of these distributions are used here
6 to represent the particle size. The highest concentrations of CCN were observed during
7 the night when they were also the most variable (Figure 2a). This is likely a result of
8 prescribed burns occurring later in the day or evening as well as a lower inversion layer
9 during the night. Interestingly, the activation ratio also follows a distinct diurnal trend
10 with $\sim 40\% \pm 20\%$ of BBA acting as CCN at 0.5% supersaturation during the night and
11 $\sim 60\% \pm 20\%$ during the day (Figure 2b). Smaller particles were typically seen during
12 the day than during the night (Figure 2c), indicating that it was the change in the particle
13 activation diameter (Figure 2d) that was responsible for this increase in daytime
14 activation ratios.



15

16 *Figure 2* The diurnal trends of a) the total cloud condensation nuclei concentration (CCNc) and particle number
17 concentration (PNc), b) the activation ratio at 0.5% supersaturation, c) the median and mode of the particle size
18 distribution and d) the apparent activation diameter. All reported values are the median of the hourly averaged data
19 for the sampling period and the error bars represent the standard deviation.

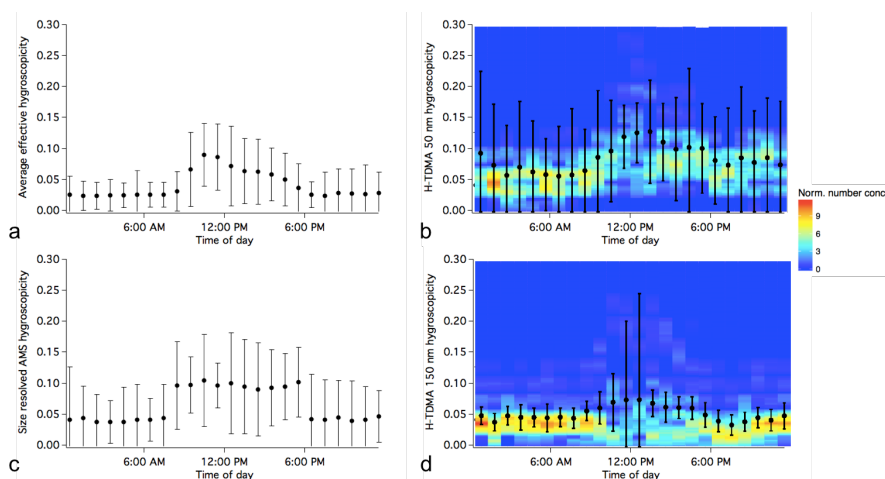
20 The hygroscopicity of BBA derived from the size-resolved AMS, CCNC/SMPS and
21 the H-TDMA followed a distinct diurnal trend (Figure 4). The CCNC-derived



1 hygroscopicity (Figure 4a) during the night time (defined as 18:00 until 07:00 local
2 time) was generally very stable and constant over the sampling period at 0.03 ± 0.03 .
3 Daytime hygroscopicity (07:00 until 18:00) was typically higher with much more
4 variability at 0.07 ± 0.05 . H-TDMA-derived hygroscopicities for 150 nm diameter
5 particles (Figure 4d) agreed very well with these values, although a much higher
6 variability was observed around noon. The hygroscopicity distributions of 50 nm
7 diameter particles followed a similar trend but were, interestingly, slightly higher than
8 the 150 nm distributions. The variability in hygroscopicity for 50 nm diameter particles
9 is much greater than for 150 nm particles, due to lower concentrations at 50 nm.
10 Hygroscopicity distributions for both 50 nm and 150 nm aerosols during the night
11 indicate a strong internal mixture of very weak hygroscopic BBA, and during the day
12 an increase and broadening of the hygroscopicity mode, suggesting an external mixture
13 of slightly more hygroscopic particles. The size-resolved AMS hygroscopicity values
14 were calculated assuming κ_{org} of 0.02 and 0.08 during the night and day, respectively.
15 The organic volume fraction was invariable (see section 3.3), therefore the increase
16 and decrease at sunrise and sunset, respectively, is driven by the choice of night and
17 day organic hygroscopicity values. These values were selected as they gave the best
18 agreement between the modelled and measured CCN concentrations, which is
19 discussed further in Section 3.4.

20

21 Literature on the diurnal variability of BBA hygroscopicity is rare. Diurnal and
22 afternoon averages of κ for BBA in the Amazonian dry season have been reported as
23 0.048 and 0.072, respectively (Gacita et al., 2016; Rissler et al., 2006; Vestin et al.,
24 2007), consistent with the results presented here. A short study (Fedele, 2015) carried
25 out in 2010 at the ATARS also reported κ values in the early dry season over a period
26 of two weeks. They showed κ values mostly between 0.05 and 0.1 for supersaturations
27 of 0.38%, 0.68% and 0.96%, with the higher values generally occurring during the day.
28 They directly measured the critical diameter and used an approximation presented in
29 Petters and Kreidenweis (2007) to calculate κ . This approximation is more appropriate
30 for κ values over 0.2, which means that the reported values between 0.05 and 0.1 were
31 slightly overestimated and would likely be more in line with the BBA hygroscopicity
32 observed in this study. Although a detailed chemical analysis was not done during that
33 study, these similar values of κ suggest that these observations could be representative
34 of early dry season fires in this region.

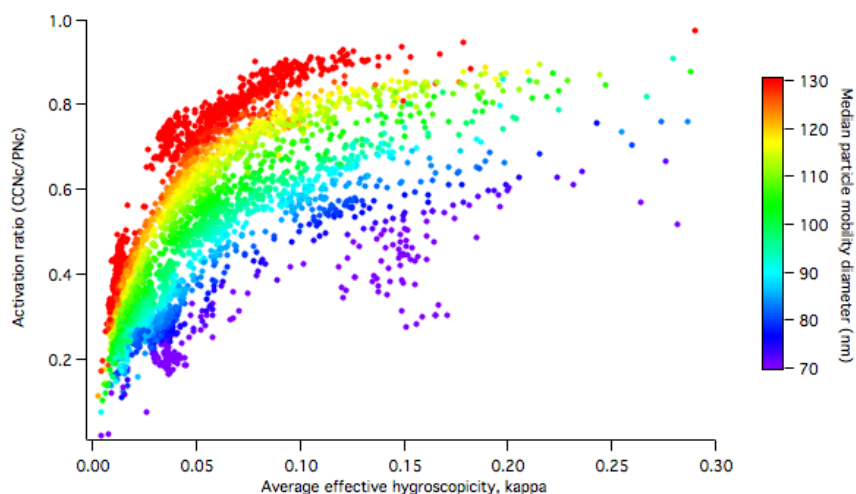


1
2
3
4
5
6
7

Figure 3 The diurnal trends of a) the CCNC-derived effective hygroscopicity parameter, b) the H-TDMA derived kelvin-corrected hygroscopicity distributions of 50 nm particles, c) the AMS-derived hygroscopicity parameter for aerodynamic diameters between 100 nm and 200 nm, assuming κ_{org} of 0.02 and 0.08 during the night and day, respectively and d) the H-TDMA derived kelvin corrected hygroscopicity distributions of 150 nm particles. The black dots on b) and d) represent the hourly median hygroscopicity values and the error bars represent the standard deviation

8 3.3 BBA composition

9 The activation ratio as a function of the effective hygroscopicity parameter, κ , as
10 calculated from equations 1 and 2, with colors indicating the median particle mobility
11 diameter, is displayed in Figure 3. This figure clearly demonstrates that both the size
12 and composition of the BBA can have a significant effect on CCN activation. For
13 example, with a constant particle size increases the CCN activation ratio from below
14 20% to above 80%. For a constant κ of 0.05 and an increase in the particle median
15 diameter from 60 nm up to 140 nm, the CCN activation ratio increases by
16 approximately 50%. The effect of composition appears to have less of an influence at
17 higher hygroscopicities, with the size being the determining factor in CCN activation
18 above a κ of 0.1. For very weakly hygroscopic ($\kappa < 0.05$) BBA, the sensitivity of particle
19 size was less prominent, with an activation ratio increase of $\sim 0.3\% \text{ nm}^{-1}$, compared to
20 a $\sim 0.7\% \text{ nm}^{-1}$ increase when $\kappa > 0.05$. These findings support the idea that cloud droplet
21 number concentrations are sensitive to composition at low hygroscopicities (Reutter et
22 al., 2009). Neglecting the effect of BBA composition in this case would lead to
23 difficulties in appropriately quantifying CCN activation.



1

2 *Figure 4 The activation ratio (CCNc/PNc) as a function of the effective hygroscopicity parameter, κ . The colours*
3 *represent the median particle mobility diameter.*

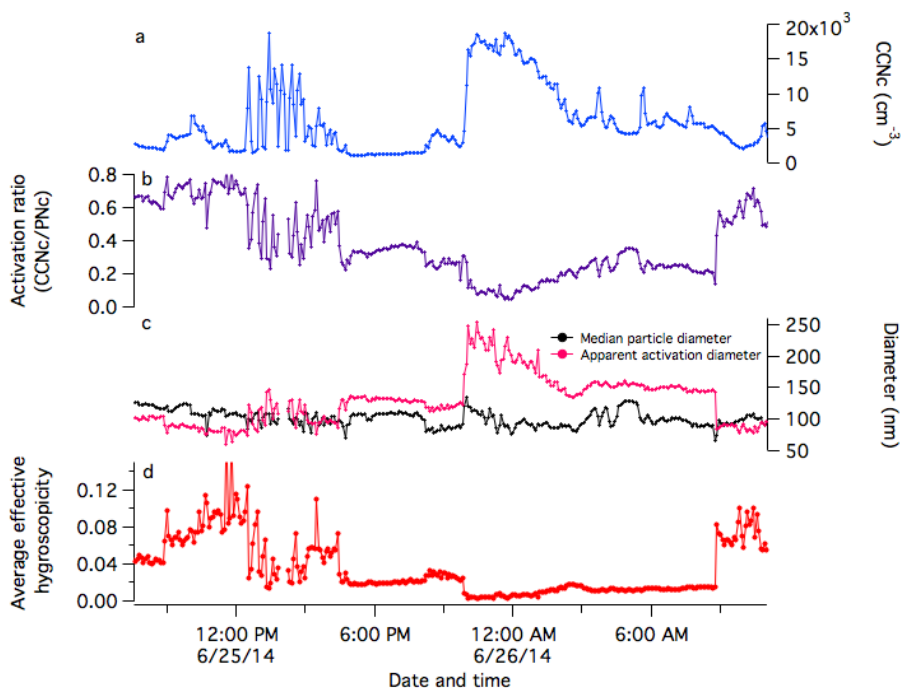
4 In order to understand the underlying causes of the variations in the hygroscopicity, the
5 size-resolved chemical composition was investigated. For bulk PM₁ composition, there
6 was a distinct increase in the inorganic mass fractions during the day due to an
7 enrichment of ammonium and sulphate species. The size-resolved composition,
8 however, revealed that these inorganic species were more present on larger particles
9 and had a $d_{\text{aerodynamic}}$ mode at approximately 350 nm, while organics had a mode at
10 approximately 250 nm. This observation is consistent with other studies that show that
11 smaller particles are more enriched with organics (Levin et al., 2014; Rose et al.,
12 2011; Gunthe et al., 2009). As the influence of composition on CCN activation is
13 irrelevant at larger sizes, it is important to investigate the composition at smaller sizes
14 where the aerosol number is highest and the composition can affect the activation
15 diameter. The size-resolved composition revealed that, within the aerodynamic
16 diameter size range of 100 nm to 200 nm, organics were completely dominant and the
17 organic volume fraction, ϵ_{org} , was invariable at approximately 90%. The total
18 hygroscopicity of BBA observed in this study was therefore predominantly influenced
19 by the organic hygroscopicity, κ_{org} . The increase in the observed hygroscopicity and
20 the inferred κ_{org} is likely a result of the photochemical oxidation of the organics. The
21 aging of biomass burning aerosol is discussed in further depth in Milic et al. (2016).

22

23 While it is likely that most of the BBA observed during the SAFIRED campaign had
24 undergone some form of aging (physical or chemical), two events provided insight into



1 the characteristics of extremely fresh BBA and are described in Mallet et al. (2016).
2 During mid-afternoon on the 25th June, grass and shrub fires were blazing ~1 km
3 southeast of the ATARS site. Wind directions during this period were very unstable
4 and frequently altering between southeasterly and northeasterly. This resulted in the
5 sampled air mass frequently changing from the "fresh" plume and more background
6 like conditions over the course of approximately 4 hours. During this time, CCN
7 concentrations varied frequently between ~2000 cm⁻³ and ~14000 cm⁻³. The activation
8 ratio, median particle size, activation diameter and hygroscopicity varied between 20%
9 and 60%, 80 nm and 110 nm, 130 nm and 80 nm and 0.02 and 0.08 respectively (see
10 Figure 5). These fires continued to blaze into the evening, slowly advancing to within
11 1 km south of the ATARS site. Due to northeasterly winds, the air mass from this fire
12 wasn't observed until approximately 10 pm that night when winds became southerly.
13 For the next four hours, CCN concentrations peaked at ~18000 cm⁻³, despite the
14 activation ratio dropping to 4%. The average effective hygroscopicity during this event
15 dropped to 0.003 and slowly increased over the period of the fire to ~0.02. This led to
16 a decrease in the apparent activation diameter from 250 nm to 150 nm, subsequently
17 increasing the CCN activation ratio to 25%. Whether this is a result of a change in the
18 burning conditions, fuel load or a combination of both is unclear. These events
19 demonstrate the importance of BB as a source of CCN, despite the relatively
20 hydrophobic nature of BBA. Furthermore, in the absence of photochemical aging, the
21 slight variation in BBA hygroscopicity during the night fire demonstrates the variability
22 of CCN activation, even over the course of an individual fire.
23



1

2 *Figure 5 The CCNc, activation ratio, median particle diameter, apparent activation diameter and average effective*
3 *hygroscopicity parameter during two periods with close proximity (<1 km) fires.*

4 The hygroscopicity of fresh and aged BBA has been studied extensively in laboratory
5 smog chambers. Some studies have shown that the photochemical oxidation of organics
6 in BBA leads to an increase in hygroscopicity (Carrico et al., 2010; Petters et al., 2009)
7 while others suggest that the hygroscopicity converges from highly ($\kappa = 0.6$) or weakly
8 ($\kappa = 0.06$) hygroscopic values to a value of approximately 0.2 ± 0.1 (Engelhart et al.,
9 2012). The observation of the close proximity fire event on the evening of the 25th of
10 June (Figure 5), as well as the diurnal trends in the calculated hygroscopicity parameter
11 (Figure 3), indicate that the composition of BBA during the night is characteristic of
12 very weakly hygroscopic fresh BBA. The increase in the hygroscopicity throughout the
13 day is due to the photochemical oxidation of organics. The high frequency of fires
14 during the early dry season in north Australia likely results in the "regional haze"
15 predominantly being composed of relatively fresh BBA with a very low hygroscopicity.
16 The aging processes were observed to increase the hygroscopicity to $\sim 0.08 \pm 0.05$,
17 which is the lower estimate of value suggested by Engelhart et al. (2012) and smaller
18 than other studies investigating BBA (Bougiatioti et al., 2016). Whether the
19 hygroscopicity would converge to higher values in the absence of frequent fires or as



1 the smoke travels away from the continent is something that needs to be explored in
2 future measurements.

3

4 **3.4 Validation of modelled CCN**

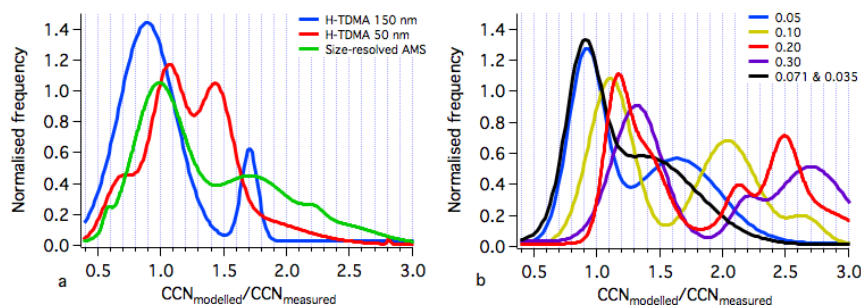
5 Detailed temporal-spatial measurements of CCN concentrations are difficult and
6 therefore assumptions must be made about the size-resolved composition and water
7 uptake for similar regions and sources. Many studies have attempted closure between
8 composition, size and CCN concentrations in order to assess the validity of these
9 assumptions (Rose et al., 2010). These studies typically agree that for most
10 environments, where hygroscopicities are moderate, the size distribution and number
11 concentration of particles are the determining factor of CCN concentrations (Dusek et
12 al., 2006). Gacita et al. (2016) however, showed that for Amazonian BBA (with
13 measured $\kappa = 0.04$), applying an assumed κ of 0.20 resulted in a 26.6% to 54.3%
14 overestimation of CCN concentrations. They suggest that κ values recommended for
15 continental and BBA are too high to describe CCN behavior of Amazonian BBA. This
16 is also the case for the SAFIRED campaign.

17

18 Figure 6 shows the normalised frequency distributions of the ratio of modelled and
19 measured CCN concentrations for five different compositional scenarios, taking into
20 account the time-dependent size distributions. For a constant hygroscopicity of 0.20,
21 daytime concentrations were overestimated by 15% to 40% while night concentrations
22 were overestimated by well over 100%. A similar case is observed for hygroscopicities
23 of 0.10 and 0.30. For an assumed constant κ of 0.05, which represents the campaign
24 average, the modelled CCN concentrations slightly underestimate the measured CCN
25 concentrations during the day by less than 10%, but overestimate the night CCN by
26 65%. Using the day and night campaign averages of 0.071 and 0.035, respectively,
27 improved the night time concentration to an overestimation of approximately 50%.
28 Using the time dependent size-resolved AMS composition and assigning and κ_{org} as
29 0.08 and 0.02 for day and night, respectively, also provides a good agreement between
30 the estimated and measured daytime CCN concentrations, but again overestimates the
31 night concentrations by 70%. H-TDMA hygroscopicity distributions showed that the
32 night was predominantly characterised by an internal mixture, suggesting that the
33 disagreement between modeled and measured CCN is due to is due to variability in fuel



1 or burning conditions of the fires and/or night time aging. The modelled CCN
2 concentrations from both the 50 nm and 150 nm H-TDMA were within 10% during the
3 day, but there were also overestimations of between 45% and 70% respectively. The
4 time resolution of the H-TDMA limited the number of CCN model calculations that
5 could be done, which introduced more potential bias for individual periods where the
6 agreement between the measured and modelled CCN was worse (or better). The
7 difficulty in sufficiently modelling night time CCN concentrations highlights the need
8 for further composition measurements of fresh BBA in this region.



9
10 *Figure 6 The normalised probability density functions for the frequency of the ratio of the modelled and measured*
11 *CCN concentrations based on a) the 150 nm and 50 nm H-TDMA derived hygroscopicities and size-resolved cToF-*
12 *AMS composition and b) the campaign average hygroscopicity, $\kappa = 0.05$, typical BB hygroscopicities of 0.1 and 0.2,*
13 *the continental average hygroscopicity of 0.3 and the day and night average effective hygroscopicity values of 0.071*
14 *and 0.035, respectively.*

15 3.5 Effect of surface tension

16 The κ values reported in this study represent the effective hygroscopicity parameter,
17 which accounts for all compositional effects on aerosol water uptake (i.e. solubility of
18 components and the reduction in surface tension to their presence). This study has
19 shown that the effective hygroscopicity parameter increases during daylight hours,
20 speculating that this is caused by the photochemical oxidation of organics. Although
21 surface tension measurements were not performed, using a value observed in a previous
22 BB study of 0.0638 Jm^{-2} (Asa-Awuku et al., 2008) in the κ -Kohler equation shows only
23 a slight decrease in hygroscopicity compared to using the surface tension of pure water
24 (Figures S2 and S3). This suggests that it is the solubility, rather than the reduction of
25 surface tension, of the organics and inorganics present in the BBA that is responsible
26 for the water uptake. On the other hand, an assumed lower estimate surface tension of
27 0.052 Jm^{-2} (Mircea et al., 2005) during the day could explain the increase in CCN
28 activation. Although models generally use the effective hygroscopicity parameter
29 (Pringle et al., 2010) due to the ease of using a single parameter, a better understanding



1 of the precise mechanisms that facilitate the uptake of water onto potential cloud
2 droplets is needed (Noziere, 2016).

3 **4 Conclusions**

4 Measurements at ATARS showed a strong link between the frequency of early dry
5 season fires and the concentrations of CCN, indicating that these fires are an important
6 source of CCN in northern Australia. The aerosol size distribution was typically
7 unimodal with a median diameter of 107 nm and the BBA was weakly hygroscopic and
8 predominately internally mixed. These conditions meant that both the composition and
9 size were important in determining the CCN activation of the BBA. A distinct diurnal
10 trend in the ratio of activated cloud condensation nuclei at 0.5% supersaturation and
11 particle number was observed, with $\sim 40\% \pm 20\%$ of BBA acting as CCN during the
12 night and $\sim 60\% \pm 20\%$ during the day. This increase in CCN activity corresponded
13 with an increase in the hygroscopicity from 0.04 ± 0.03 to 0.07 ± 0.05 . This was likely
14 due to the daytime photochemical oxidation of organic compounds within BBA. While
15 not investigated in this study, this smoke has the potential to penetrate into the upper
16 levels of the troposphere, particularly as the dry season progresses, and it also flows
17 over the Timor Sea where change in cloud albedo and lifetime is likely to be sensitive
18 to CCN concentration changes. In the case of northern Australian dry season fires,
19 assuming typical continental hygroscopicities of 0.10, 0.20 and 0.30 led to CCN
20 overestimates of 10% to 30% during the day and 100% to over 150% during the night.
21 It is therefore important that the CCN activation can be better modelled.

22

23 BBA related CCN concentrations are likely to be further enhanced throughout the dry
24 season as temperatures increase and there are more frequent fires. Long term
25 monitoring or future measurements later in the dry season would allow a more detailed
26 analysis into the seasonal relationship between fire frequency, intensity and CCN.
27 Other aerosol-cloud interactions are likely to change as the season progresses. Higher
28 solar radiation and relative humidity during the late dry season lead to the formation of
29 pyro-cumulous clouds and higher rainfall in comparison to the early dry season
30 (Bowman et al., 2007). Concurrent aircraft measurements would be required to
31 investigate the penetration and evolution of smoke into upper levels of the troposphere.
32 Characterising the presence of smoke within, below and above clouds is required to
33 fully understand the vertical radiative effect of these fires. The south easterly trade



1 winds carry this smoke over waters in the Indian and western Pacific oceans known as
2 the tropical warm pool. Measurements in Indonesia or on a ship in the Timor Sea would
3 therefore also be useful in determining the long-range transport and evolution of the
4 smoke. Furthermore, a mobile sampling chamber positioned downwind of prescribed
5 burns that occur in this region, both during the day and night, would be beneficial in
6 understanding the variability of the composition of freshly emitted BBA.

7 **Data availability**

8 Data can be accessed upon request to the corresponding author (Branka Miljevic;
9 b.miljevic@qut.edu.au)

10 **Author contributions**

11 Marc Mallet wrote the manuscript, designed and conducted experimental work and
12 analysed and interpreted data. Luke Cravigan contributed to writing the manuscript,
13 data analysis and data interpretation. Anđelija Milic analysed data and reviewed the
14 manuscript. Joel Alroe designed experimental work, analysed data and reviewed the
15 manuscript, Zoran Ristovski designed experimental work and reviewed the manuscript.
16 Jason Ward designed experimental work and conducted experimental work, Melita
17 Keywood led the SAFIRED campaign and reviewed the manuscript, Leah Williams
18 contributed to the experimental work and reviewed the manuscript, Paul Selleck
19 designed experimental work and analysed data, Branka Miljevic designed and
20 conducted experimental work and reviewed the manuscript.

21 **References**

- 22 Andersen, A. N., Cook, G. D., Corbett, L. K., Douglas, M. M., Eager, R. W., Russell-
23 Smith, J., Setterfield, S. A., Williams, R. J., and Woinarski, J. C.: Fire frequency and
24 biodiversity conservation in Australian tropical savannas: implications from the
25 Kapalga fire experiment, *Austral Ecology*, 30, 155-167, 2005.
- 26 Andreae, M., Artaxo, P., Fischer, H., Freitas, S., Grégoire, J. M., Hansel, A., Hoor, P.,
27 Kormann, R., Krejci, R., and Lange, L.: Transport of biomass burning smoke to the
28 upper troposphere by deep convection in the equatorial region, *Geophysical Research*
29 *Letters*, 28, 951-954, 2001.
- 30 Asa-Awuku, A., Sullivan, A., Hennigan, C., Weber, R., and Nenes, A.: Investigation
31 of molar volume and surfactant characteristics of water-soluble organic compounds in
32 biomass burning aerosol, *Atmospheric Chemistry and Physics*, 8, 799-812, 2008.
- 33 Bond, T. C., and Bergstrom, R. W.: Light absorption by carbonaceous particles: An
34 investigative review, *Aerosol science and technology*, 40, 27-67, 2006.
- 35 Bougiatioti, A., Bezantakos, S., Stavroulas, I., Kalivitis, N., Kokkalis, P., Biskos, G.,
36 Mihalopoulos, N., Papayannis, A., and Nenes, A.: Biomass-burning impact on CCN



- 1 number, hygroscopicity and cloud formation during summertime in the eastern
2 Mediterranean, *Atmospheric Chemistry and Physics*, 16, 7389-7409, 2016.
- 3 Bowman, D., and Vigilante, T.: Conflagrations: the culture, ecology and politics of
4 landscape burning in the north Kimberley, *Ngoonjook*, 38, 2001.
- 5 Bowman, D. M., Dingle, J. K., Johnston, F. H., Parry, D., and Foley, M.: Seasonal
6 patterns in biomass smoke pollution and the mid 20th - century transition from
7 Aboriginal to European fire management in northern Australia, *Global Ecology and*
8 *Biogeography*, 16, 246-256, 2007.
- 9 Carrico, C., Petters, M., Kreidenweis, S., Sullivan, A., McMeeking, G., Levin, E.,
10 Engling, G., Malm, W., and Collett Jr, J.: Water uptake and chemical composition of
11 fresh aerosols generated in open burning of biomass, *Atmospheric Chemistry and*
12 *Physics*, 10, 5165-5178, 2010.
- 13 Carslaw, K., Boucher, O., Spracklen, D., Mann, G., Rae, J., Woodward, S., and
14 Kulmala, M.: A review of natural aerosol interactions and feedbacks within the Earth
15 system, *Atmospheric Chemistry and Physics*, 10, 1701-1737, 2010.
- 16 Chen, H., Sangster, J., Teng, T., and Lenzi, F.: A general method of predicting the water
17 activity of ternary aqueous solutions from binary data, *The Canadian Journal of*
18 *Chemical Engineering*, 51, 234-241, 1973.
- 19 Dirksen, R. J., Folkert Boersma, K., De Laat, J., Stammes, P., Van Der Werf, G. R.,
20 Val Martin, M., and Kelder, H. M.: An aerosol boomerang: Rapid around - the - world
21 transport of smoke from the December 2006 Australian forest fires observed from
22 space, *Journal of Geophysical Research: Atmospheres*, 114, 2009.
- 23 Dusek, U., Frank, G., Hildebrandt, L., Curtius, J., Schneider, J., Walter, S., Chand, D.,
24 Drewnick, F., Hings, S., and Jung, D.: Size matters more than chemistry for cloud-
25 nucleating ability of aerosol particles, *Science*, 312, 1375-1378, 2006.
- 26 Engelhart, G., Hennigan, C., Miracolo, M., Robinson, A., and Pandis, S. N.: Cloud
27 condensation nuclei activity of fresh primary and aged biomass burning aerosol,
28 *Atmospheric Chemistry and Physics*, 12, 7285-7293, 2012.
- 29 Fedele, R. M.: Observations of Australian Cloud Condensation Nuclei (CCN), RMIT
30 University, 2015.
- 31 Gunthe, S. S., King, S. M., Rose, D., Chen, Q., Roldin, P., Farmer, D. K., Jimenez, J.
32 L., Artaxo, P., Andreae, M. O., Martin, S. T., and Pöschl, U.: Cloud condensation nuclei
33 in pristine tropical rainforest air of Amazonia: size-resolved measurements and
34 modeling of atmospheric aerosol composition and CCN activity, *Atmospheric*
35 *Chemistry and Physics*, 9, 7551-7575, 2009.
- 36 Gysel, M., McFiggans, G., and Coe, H.: Inversion of tandem differential mobility
37 analyser (TDMA) measurements, *Journal of Aerosol Science*, 40, 134-151, 2009.
- 38 Johnson, G. R., Ristovski, Z., and Morawska, L.: Method for measuring the
39 hygroscopic behaviour of lower volatility fractions in an internally mixed aerosol,
40 *Journal of Aerosol Science*, 35, 443-455, 2004.
- 41 Kaufman, Y., Hobbs, P., Kirchhoff, V., Artaxo, P., Remer, L., Holben, B., King, M.,
42 Ward, D., Prins, E., and Longo, K.: Smoke, Clouds, and Radiation - Brazil (SCAR -
43 B) experiment, *Journal of Geophysical Research: Atmospheres*, 103, 31783-31808,
44 1998.
- 45 Kondo, Y., Takegawa, N., Miyazaki, Y., Ko, M., Koike, M., Kita, K., Kawakami, S.,
46 Shirai, T., Ogawa, T., and Blake, D. R.: Effects of biomass burning and lightning on
47 atmospheric chemistry over Australia and South-east Asia, *International Journal of*
48 *Wildland Fire*, 12, 271-281, 2003.
- 49 Lawson, S. J., Keywood, M. D., Galbally, I. E., Gras, J. L., Caine, J. M., Cope, M. E.,
50 Krummel, P. B., Fraser, P. J., Steele, L. P., Bentley, S. T., Meyer, C. P., Ristovski, Z.,



- 1 and Goldstein, A. H.: Biomass burning emissions of trace gases and particles in marine
2 air at Cape Grim, Tasmania, *Atmospheric Chemistry and Physics*, 15, 13393-13411,
3 2015.
- 4 Levin, E., Prenni, A., Palm, B., Day, D., Campuzano-Jost, P., Winkler, P., Kreidenweis,
5 S., DeMott, P., Jimenez, J., and Smith, J.: Size-resolved aerosol composition and its
6 link to hygroscopicity at a forested site in Colorado, *Atmospheric Chemistry and*
7 *Physics*, 14, 2657-2667, 2014.
- 8 Mallet, M. D., Desservettaz, M. J., Miljevic, B., Milic, A., Ristovski, Z. D., Alroe, J.,
9 Cravigan, L. T., Jayaratne, E. R., Paton-Walsh, C., Griffith, D. W. T., Wilson, S. R.,
10 Kettlewell, G., van der Schoot, M. V., Selleck, P., Reisen, F., Lawson, S. J., Ward, J.,
11 Harnwell, J., Cheng, M., Gillett, R. W., Molloy, S. B., Howard, D., Nelson, P. F.,
12 Morrison, A. L., Edwards, G. C., Williams, A. G., Chambers, S. D., Werczynski, S.,
13 Williams, L. R., Winton, V. H. L., Atkinson, B., Wang, X., and Keywood, M. D.:
14 Biomass burning emissions in north Australia during the early dry season: an overview
15 of the 2014 SAFIRED campaign, *Atmospheric Chemistry and Physics*, 2016,
16 submitted.
- 17 Milic, A., Mallet, M. D., Cravigan, L. T., Alroe, J., Ristovski, Z. D., Selleck, P.,
18 Lawson, S. J., Ward, J., Desservettaz, M. J., Paton-Walsh, C., Williams, L. R.,
19 Keywood, M. D., and Miljevic, B.: Aging of aerosols emitted from biomass burning in
20 northern Australia, *Atmospheric Chemistry and Physics Discussions*, 2016, 1-24,
21 10.5194/acp-2016-730, 2016.
- 22 Mircea, M., Facchini, M., Decesari, S., Cavalli, F., Emblico, L., Fuzzi, S., Vestin, A.,
23 Rissler, J., Swietlicki, E., and Frank, G.: Importance of the organic aerosol fraction for
24 modeling aerosol hygroscopic growth and activation: a case study in the Amazon Basin,
25 *Atmospheric Chemistry and Physics*, 5, 3111-3126, 2005.
- 26 Mochida, M., and Kawamura, K.: Hygroscopic properties of levoglucosan and related
27 organic compounds characteristic to biomass burning aerosol particles, *Journal of*
28 *Geophysical Research: Atmospheres* (1984–2012), 109, 2004.
- 29 Novakov, T., and Corrigan, C.: Cloud condensation nucleus activity of the organic
30 component of biomass smoke particles, *Geophysical Research Letters*, 23, 2141-2144,
31 1996.
- 32 Noziere, B.: Don't forget the surface, *Science*, 351, 1396-1397, 2016.
- 33 Petters, M., and Kreidenweis, S.: A single parameter representation of hygroscopic
34 growth and cloud condensation nucleus activity, *Atmospheric Chemistry and Physics*,
35 7, 1961-1971, 2007.
- 36 Petters, M. D., Carrico, C. M., Kreidenweis, S. M., Prenni, A. J., DeMott, P. J., Collett,
37 J. L., and Moosmüller, H.: Cloud condensation nucleation activity of biomass burning
38 aerosol, *Journal of Geophysical Research: Atmospheres*, 114, 2009.
- 39 Platnick, S., and Twomey, S.: Determining the susceptibility of cloud albedo to changes
40 in droplet concentration with the Advanced Very High Resolution Radiometer, *Journal*
41 *of Applied Meteorology*, 33, 334-347, 1994.
- 42 Pöschl, U., Rose, D., and Andreae, M. O.: Climatologies of Cloud-related Aerosols.
43 Part 2: Particle Hygroscopicity and Cloud Condensation Nucleus Activity, in: *Clouds*
44 *in the Perturbed Climate System: Their Relationship to Energy Balance, Atmospheric*
45 *Dynamics, and Precipitation*, MIT Press, 58-72, 2009.
- 46 Pringle, K., Tost, H., Pozzer, A., Pöschl, U., and Lelieveld, J.: Global distribution of
47 the effective aerosol hygroscopicity parameter for CCN activation, *Atmospheric*
48 *Chemistry and Physics*, 10, 5241-5255, 2010.



- 1 Reid, J., Koppmann, R., Eck, T., and Eleuterio, D.: A review of biomass burning
2 emissions part II: intensive physical properties of biomass burning particles,
3 Atmospheric Chemistry and Physics, 5, 799-825, 2005.
- 4 Ristovski, Z. D., Wardoyo, A. Y., Morawska, L., Jamriska, M., Carr, S., and Johnson,
5 G.: Biomass burning influenced particle characteristics in Northern Territory Australia
6 based on airborne measurements, Atmospheric Research, 96, 103-109, 2010.
- 7 Rose, D., Nowak, A., Achtert, P., Wiedensohler, A., Hu, M., Shao, M., Zhang, Y.,
8 Andreae, M., and Pöschl, U.: Cloud condensation nuclei in polluted air and biomass
9 burning smoke near the mega-city Guangzhou, China–Part 1: Size-resolved
10 measurements and implications for the modeling of aerosol particle hygroscopicity and
11 CCN activity, Atmospheric Chemistry and Physics, 10, 3365-3383, 2010.
- 12 Rose, D., Gunthe, S. S., Su, H., Garland, R. M., Yang, H., Berghof, M., Cheng, Y. F.,
13 Wehner, B., Achtert, P., Nowak, A., Wiedensohler, A., Takegawa, N., Kondo, Y., Hu,
14 M., Zhang, Y., Andreae, M. O., and Pöschl, U.: Cloud condensation nuclei in polluted
15 air and biomass burning smoke near the mega-city Guangzhou, China–Part 2: Size-
16 resolved aerosol chemical composition, diurnal cycles, and externally mixed weakly
17 CCN-active soot particles, Atmospheric Chemistry and Physics, 11, 2817-2836, 2011.
- 18 Spracklen, D., Carslaw, K., Pöschl, U., Rap, A., and Forster, P.: Global cloud
19 condensation nuclei influenced by carbonaceous combustion aerosol, Atmospheric
20 Chemistry and Physics, 11, 9067-9087, 2011.
- 21 Stokes, R., and Robinson, R.: Interactions in aqueous nonelectrolyte solutions. I.
22 Solute-solvent equilibria, The Journal of Physical Chemistry, 70, 2126-2131, 1966.
- 23 Twomey, S.: Aerosols, clouds and radiation, Atmospheric Environment. Part A.
24 General Topics, 25, 2435-2442, 1991.
- 25 van der Werf, G. R., Randerson, J. T., Giglio, L., Collatz, G. J., Kasibhatla, P. S., and
26 Arellano Jr, A. F.: Interannual variability in global biomass burning emissions from
27 1997 to 2004, Atmospheric Chemistry and Physics, 6, 3423-3441, 2006.
- 28 Ward, D., Kloster, S., Mahowald, N., Rogers, B., Randerson, J., and Hess, P.: The
29 changing radiative forcing of fires: global model estimates for past, present and future,
30 Atmospheric Chemistry and Physics, 12, 2012.
- 31 Warner, J., and Twomey, S.: The production of cloud nuclei by cane fires and the effect
32 on cloud droplet concentration, Journal of the Atmospheric Sciences, 24, 704-706,
33 1967.
- 34
35